Local motion effects on form in radial frequency patterns

James Edwin Dickinson School of Psychology, University of Western Australia, Perth, WA, Australia

Limin Han School of Psychology, University of Western Australia, Perth, WA, Australia

Jason Bell School of Psychology, University of Western Australia, Perth, WA, Australia, & McGill Vision Research, Department of Ophthalmology, McGill University, Montreal, Quebec, Canada

David R. Badcock School of Psychology, University of Western Australia, Perth, WA, Australia

Sinusoidal modulation of radial speed around a circular path of tangentially oriented Gabor patches results in the percept of modulation of the radius. These patterns have been called motion radial frequency (RF) patterns. Sensitivity to these patterns has been attributed to global summation of local speed by mechanisms, analogous to those proposed to explain sensitivity to spatial RF patterns, which are sensitive to particular radial frequencies of speed modulation. We demonstrate that: Adaptation to spatial RF patterns results in a phase specific after effect in motion RF patterns and vice versa; the rate of change of perceived displacement of a Gabor patch with a moving grating with increasing speed of that grating, is independent of whether the patch is or is not incorporated into a circular path; in the absence of local motion direction cues, global integration across 1, 2 and 3 cycles of motion and spatial RF modulation conforms to a power function with the same index; and finally that the magnitude of the motion position illusion is sufficient and necessary to account for sensitivity to motion RF patterns. We therefore propose that motion RF patterns are analyzed by the same mechanisms responsible for sensitivity to spatial RF patterns using perceived rather than actual local positions of the Gabor patches.

Keywords: global form, motion position illusion

Citation: Dickinson, J. E., Han, L., Bell, J., & Badcock, D. R. (2010). Local motion effects on form in radial frequency patterns. *Journal of Vision, 10*(3):20, 1–15, http://journalofvision.org/10/3/20/, doi:10.1167/10.3.20.

Introduction

Visual information facilitates interaction of an observer with their environment. Parsing of the scene into identifiable objects allows an internal model of the environment to be built to enable the observer to plan a course of action. The shape, or form, of an object plays an important role in its identification (Biederman, 1987).

Objects often subtend large visual angles at the observer and so the processing of objects can be considered hierarchical in the sense that information from local spatial and temporal filters is pooled in the analysis of form. At the earliest level of cortical processing of visual information the local filters are tuned, spatially, for a change in luminance or luminance contrast across a boundary and, temporally, for the sense of the direction of motion of that boundary (De Valois, Cottaris, Mahon, Elfar, & Wilson, 2000; Hubel & Wiesel, 1968). Local spatial filters associate with adjacent and approximately collinear filters (Field, Hayes, & Hess, 1993; Li & Gilbert, 2002) to signal paths. Closed paths, which may circumscribe objects, segregate spontaneously from the background (Kovacs & Julesz, 1993). The boundaries of objects which are not characterized by a change in luminance can be revealed as boundaries between regions of dissimilar texture or regions of similar texture in relative motion (Regan & Hamstra, 1992). Once the boundary of an object is revealed its shape can usually be encoded.

Humans are very sensitive to subtle differences between shapes of objects (Loffler, Wilson, & Wilkinson, 2003). Performance in discriminating a circle from a similar pattern deformed by a small sinusoidal modulation of its radius as a function of polar angle can qualify as a hyperacuity in that radial deformation can be detected that is smaller than the sampling interval of the image on the retina (Wilkinson, Wilson, & Habak, 1998).

Recent studies (Bell & Badcock, 2009; Bell, Badcock, Wilson, & Wilkinson, 2007; Loffler et al., 2003) show that spatial information is pooled across cycles of deformation in the detection of low frequencies of sinusoidal modulation of the radius. For these so called spatial form radial

doi: 10.1167/10.3.20 Received September 10, 2009; published March 31, 2010 ISSN 1534-7362

frequency (spatial RF) patterns, shapes defined by 3, 4 or 5 cycles of modulation around the closed path (RF3, RF4 or RF5 patterns) exhibited global pooling of information across cycles, while frequencies of 10 or higher did not. Sensitivity to higher frequency spatial RF patterns could be accounted for by the probability of detection of one of the total number of cycles of deformation and can therefore be ascribed to local rather than global processes.

For spatial RF patterns the form of the stimulus is explicit in the bounding luminance-defined path. However, global pooling of local motion information can also result in a percept of form. Psychophysical experiments have shown orientation discrimination performance to be comparable for bars in random dot patterns defined by luminance and motion contrast (Regan & Hamstra, 1992). Regan and Hamstra (1992) proposed that the output of local motion filters is passed to form filters which then delineate a boundary. Rainville and Wilson (2004, 2005), however, introduced an ingenious stimulus which allows RF modulation of spatial and motion cues to be manipulated independently. A circle of tangentially aligned Gabor patches provides a template. To produce a spatial RF pattern a radial displacement, sampled from the appropriate frequency sinusoid, is applied to the position of each Gabor patch. The orientation of the grating within the patch is tangential to the path. A motion RF pattern is created by causing the grating within each Gabor patch on the circle to move radially with a speed sampled from a sinusoidal speed distribution. The perceived form of the motion RF patterns approximates that of the spatial RF patterns despite the fact that the centers of the Gabor patches lie on a circle. Rainville and Wilson (2004, 2005) demonstrated that signal integration over increasing numbers of cycles of speed modulation in motion defined RF patterns was steeper than linear, which implies a synergistic (i.e. multiplicative) process. This compares with additive summation across cycles of deformation for spatial RF patterns (Loffler et al., 2003). These differing patterns of integration led them to propose a high level cortical mechanism that globally integrates motion cues over space and is sensitive to a modulation of speed around a circle. They also demonstrated that the effects of motion RF pedestals on sensitivity to spatial RF patterns and vice versa were detrimental, showing the spatial form and motion form systems to be antagonistic. There is some evidence in their data, however, that when the pedestal RF modulation was in phase with the test RF modulation, sensitivities conformed to the 'dipper function' characteristic of increment detection within a single channel (Bell, Wilkinson, Wilson, Loffler, & Badcock, 2009; Nachmias & Sansbury, 1974). Moreover, it has previously been shown that at the level of the local spatio-temporal filters the effect of local motion cannot be dissociated from perceived position. The perceived position of the Gaussian window of a stationary Gabor patch is displaced in the direction of motion of its windowed grating (De Valois & De Valois, 1991) and Hayes (2000) showed that it is the apparent position of Gabor contour elements that governs binding into a path rather than their actual position. The effects of motion on perceived position are local but if speed were modulated sinusoidally around a circle the resulting local displacements would give the impression of spatial form in phase with the speed modulation. Adaptation to spatial RF patterns has been shown to result in a subsequently presented circle appearing to have the opposite phase of modulation (Anderson, Habak, Wilkinson, & Wilson, 2007), therefore motion RF patterns should give rise to opposite phase after effects in low amplitude spatial RF patterns and vise versa. Our hypothesis, that the perception of motion-defined form arises from the integration of positions perceived as displaced in the direction of local motion is supported by a series of five experiments giving the following five results.

1. Brief exposure to spatial RF patterns results in a persistent spatial RF after effect with the opposite phase of modulation.
2. Exposure to motion RF patterns results in a phase specific after effect which modifies the perceived form of subsequently presented spatial RF patterns.
3. Brief exposure to a spatial RF pattern results in an after effect with the capacity to null the apparent deformation of a motion RF pattern of the same phase of modulation.
4. The rate of change of perceived displacement of a Gabor patch with speed of the moving grating is independent of whether the patch is or is not incorporated into a motion RF pattern.
5. In the absence of local motion direction cues, which provide a local cue with which to discriminate test and reference stimuli, the summation index across multiple lobes of RF patterns is the same for motion and spatial RF patterns.

We therefore propose a modification of Rainville and Wilson's model; that the perception of motion induced form in motion RF patterns is due to integration, in the form system, of perceived local position modified by the motion position illusion, rather than modification of global form by a mechanism sensitive to global modulation of speed around a circle. Our interpretation is confirmed by the demonstration that RF form is not perceived in motion RF patterns composed of hard-edged patches on a dark (<0.5 cd/m^2) background that do not support the motion position illusion.

Methods

Apparatus

Custom stimuli were created using Matlab 6.5 (Mathworks, Natick, MA, USA) on a PC and drawn from the frame buffer

of a Cambridge Research Systems 2/5 visual stimulus generator to a Sony Trinitron G420 monitor. Screen resolution was 1024 × 768 pixels with each pixel subtending 1′ of visual angle at a viewing distance of 115 cm. The viewing distance was stabilized through the use of a chinrest. Screen refresh rate was 100 Hz. Background luminance of the stimuli was 45 cd/m^2 and the screen was viewed in a darkened room with an ambient luminance of <1 cd/m^2. Luminance calibration was performed using an Optical OP200-E photometer (head model number 265), and associated software (Cambridge Research Systems). A button box was used to record observer responses.

Observers

Five experienced psychophysical observers participated. JB, LH and ED are authors; RO and VB were naïve to the purpose of the experiments. All had normal or corrected to normal visual acuity.

Stimuli

Stimuli were closed paths of Gabor patches (except for a particular condition of Experiment 5, described in the Results section, where the patches had hard edges). The maximum Michelson luminance contrast was 1 (maximum luminance 90 cd/m^2). Patterns had a background luminance of 45 cd/m^2 except for the hard edged condition of Experiment 5 where the background was dark (<0.5 cd/m^2). The form of the path was deformed from circular either physically, by sinusoidally modulating the radius of the path around the circle, or perceptually, through the introduction of a sinusoidal radial speed profile to the gratings of the Gabor patches. Such patterns are referred to as spatial (Loffler et al., 2003) and motion (Rainville & Wilson, 2004, 2005) radial frequency (RF) patterns respectively. The circular patterns had a radius of 4° (2° for Experiment 5) of visual angle. In the spatial RF patterns this radius was modulated by a sine function with a frequency of 3 cycles per 2π radians. The radius of the spatial RF pattern, $R(\theta)$, is given by Equation 1 below.

$$R(\theta) = R_0 \times (1 + A \times \sin(3\theta + \varphi)), \quad (1)$$

R_0 is the un-modulated circle radius, A is the modulation amplitude (defined as a fraction of R_0), θ is the polar angle relative to the x axis and φ the phase of the sinusoid. Modulated patterns always had three vertices. For a phase of zero the pattern would appear to be resting on a vertex and for a phase of π radians it would be resting on a side. The gratings of the Gabor patches comprising the path were tangential to the path for all phases and amplitudes.

The path of Gabor patches in the motion RF patterns was circular with a radius of 4° (2° for Experiment 5) of visual angle. The gratings of the Gabor patches were oriented tangential to this circle. The gratings of the patches drifted with a radial speed given by Equation 2 below.

$$S(\theta) = S_0 \times \sin(3\theta + \varphi) + S_{d.c.}, \quad (2)$$

where S_0 is the amplitude of the speed modulation, θ is the polar angle, φ is the phase of the sinusoid and $S_{d.c.}$ is a constant speed component. $S_{d.c.}$ had a value of zero for all experiments other than Experiment 5 when it was 0.5°/s. The motion defined RF patterns, despite having no spatial deformation, had the same appearance as the spatial RF patterns of resting on a vertex (phase zero) or a side (phase π radians).

Experimental procedures

Observers in Experiments 1, 2 and 3 were required to report whether they perceived a test stimulus to be resting on a vertex (phase zero) or a side (phase π radians), a single interval forced choice (SIFC) task. The method of constant stimuli was adopted, sampling 9 points on the psychometric function. The data were fitted by a cumulative normal distribution yielding a point of subjective equality (where the test stimulus would be perceived as circular). Experiments 1, 2 and 3 examined the effects of adapting stimuli presented prior to the test stimuli. The adapting and test stimuli could be spatial or motion RF patterns. The experimental details of each experiment are presented individually in the Results section.

Experiments 4 and 5 differed in procedure. Experiment 4 was an alignment task where observers were required to report whether a central Gabor patch was to the left or right on an imaginary line joining two vertically arranged reference patches 4° to the right of and 5° above and below a central fixation point. The gratings within the reference Gabor patches were vertical, matching the orientation of the target patch for optimum performance (Keeble & Nishida, 2001). The method of constant stimuli was used to sample seven displacements of the reference patches relative to the central patch and the resulting psychometric data were fitted by a cumulative normal distribution. Points of subjective alignment were derived for a range of grating speeds for conditions where the central patch was presented as a component part of an RF3 path (with a phase of π/2 radians) or alone. Experiment 5 repeated Rainville and Wilson's integration experiment across 1, 2 and 3 cycles of spatial and motion RF3 modulation but with patterns incorporating a d.c. component in the speed distribution

to remove local direction of motion (centrifugal vs. centripetal) differences. In a two interval forced choice (2IFC) task observers were required to discriminate a deformed test pattern from a reference circle. The test patterns were deformed by 1, 2 or 3 cycles of modulation of an RF3 pattern. The method of constant stimuli was employed using seven amplitudes of deformation. A Quick function was fitted to the data describing the probability of correct identification of the deformed stimulus running from a probability of 0.5 to a probability of 1. The 75% correct performance level was adopted as the threshold for discrimination. The experiment was repeated using patterns composed of patches with hard edges (rectangular rather than Gaussian profiles for the maximum luminance contrast of the gratings) on a dark background (<0.5 cd/m^2). Alignment tasks analogous to the single patch condition of Experiment 4 were performed using the Gaussian profile and hard edged patches to provide transfer functions relating grating speed to perceived patch displacement due to the motion position illusion. These transfer functions were applied to the motion RF patterns to predict perceived spatial modulation amplitudes for the patterns, for comparison with actual spatial RF thresholds.

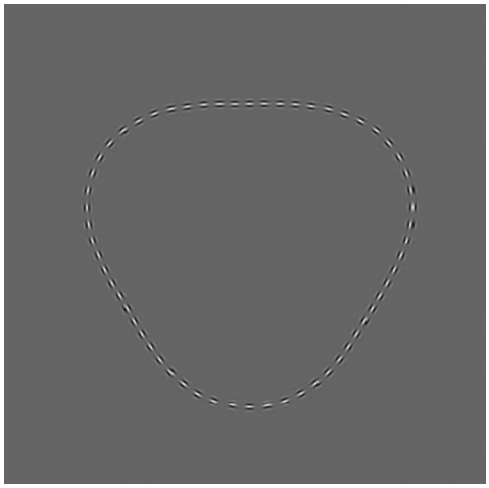

Movie 1. An example trial from Experiment 1. The observer adapts to a spatial RF pattern with a zero phase and amplitude of 0.1. The subsequently displayed test pattern, a circle in this example, is perceived as distorted from its actual shape with a modulation opposite in phase to the adaptor. The adaptor in this example is presented for 160 ms and the test stimulus persists for 160 ms after an ISI of 640 ms.

Results

Experiment 1: Brief exposure to spatial RF patterns results in a persistent spatial RF after effect with the opposite phase of modulation

The purpose of this experiment was to establish the time course of the induction and decay of the spatial after effect of adaptation to spatial RF patterns. Two sets of conditions used spatial RF pattern adaptors and spatial RF pattern test stimuli. The first set examined the effect of the duration of the adapting stimulus on perception of the test stimulus. The second measured the rate of decay of the adaptation effect. Both the adapting stimuli and the test stimuli were composed of 60 Gabor patches arranged on equally spaced radii. The diameter of the Gaussian envelopes of the Gabor patches was 9.4′ of visual angle at half maximum amplitude, spatial frequency of the gratings was 8 cycles per degree (c/°) and the mean radius of the patterns was 4° of visual angle. The adapting stimulus always had a phase (φ) of zero and an amplitude (A in Equation 1) of 0.1. In the first set of conditions the duration of presentation of the adaptor was varied within the range 20 to 640 ms. A constant inter stimulus interval (ISI) of 640 ms was used and the test stimulus was displayed for 160 ms. An example trial is illustrated in Movie 1.

For each condition the amplitude of the test spatial RF pattern was varied to sample 9 points on the psychometric function. The point of subjective equality (percept of an undistorted circle) yielded the amplitude of the spatial RF pattern test stimulus required to null the spatial RF after effect induced by the adaptor. A baseline, no adaptor, condition was also run for each observer and subtracted from the PSEs to give a genuine measure of the magnitude of the after effect. Results for this first set of conditions are displayed in Figure 1.

The adaptation effect is almost saturated at an adaptor duration of 40 ms. The adaptor had an amplitude of 0.1 times the pattern radius and so the magnitude of the adaptation effect was around 20–30% of the adaptor amplitude. The phase of the test stimulus required to null the after effect was the same as the adaptor demonstrating that the after effect is phase specific and is of opposite phase to the adaptor. A duration of 160 ms was used for all subsequent applications of a spatial RF pattern adaptor.

In the second set of conditions the adaptor duration, prior to each trial, was held constant at 160 ms and the ISI was varied between 160 and 5120 ms. The experimental paradigm and treatment of the results was the same as for the first set of conditions. The results for these conditions are displayed in Figure 2. The amplitude of deformation at the PSE for the un-adapted condition has again been removed from these data. A power function ($A = Const \times ISI^{\gamma}$) is a good fit to the entire data set of each of the observers (γ: ED = −0.31; LH = −0.11; RO = −0.13;

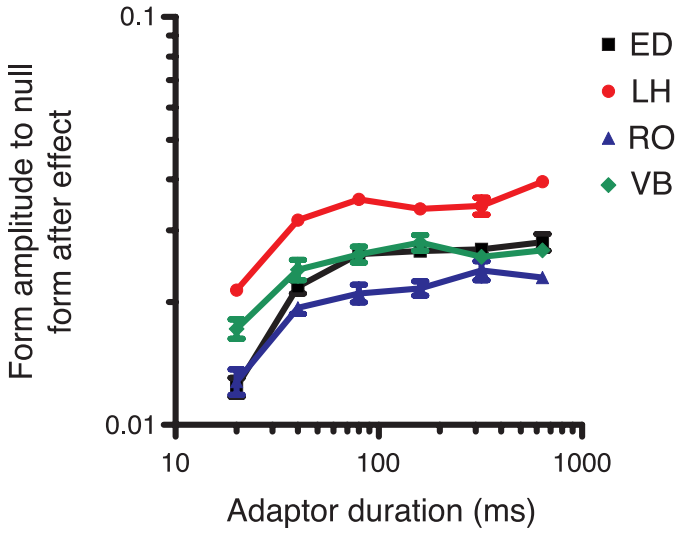

Figure 1. Rise time of the spatial form after effect. The graph shows the amplitude of the spatial RF pattern test stimulus required to null the effect of adaptation to a spatial RF pattern stimulus of the same phase and amplitude of 0.1 for a range of adaptor durations. The error bars are 95% confidence intervals.

VB = −0.10), revealing long lasting (slowly decaying) after effects of even this short period of adaptation.

Experiment 2: Exposure to motion RF patterns results in a phase specific after effect which modifies the perceived form of subsequently presented spatial RF patterns

The second experiment investigated whether a motion defined RF pattern induced an after effect in a spatially defined RF pattern. Rainville and Wilson (2004) showed that thresholds for discriminating a spatial RF pattern from a circular path are increased in the presence of both in phase and out of phase motion RF pedestals. They conclude that this is indicative of a high level interference between motion and form processing pathways. In this interpretation, adaptation to a motion RF might conceivably result in a phase specific motion RF after effect which would interfere with the form processing, but this would not result in a perceived deformation of a circle in opposite phase to the adaptor. Conversely, if the form apparent in the motion RF pattern is due to local displacements in perceived positions of the patches, due to the motion position illusion, then the global form perceived would be that of a spatial RF pattern and a phase specific after effect would result.

The adapting motion RF pattern comprised 28 frames of 50 ms duration, a total adaptor duration of 1.4 seconds. The starting phase of the grating of each Gabor patch was assigned at random. The spatial RF test pattern followed a 160 ms ISI and was displayed for 160 ms. The experiment was duplicated using Gabor patches with gratings of two different spatial frequencies, 8 c/° and 2 c/°. Stimuli composed of patches with 8 c/° gratings contained 60 patches with a diameter at half height of 9.4′ and those composed of patches with 2 c/° gratings contained 18 patches with a diameter at half height of 37.6′. Maximum speed for the gratings of the Gabor patches, S_0, was 2.288 wavelengths per second, which corresponds to 0.286°/s for the higher spatial frequency stimuli and 1.144°/s for the lower. A particular cycle in an 8 c/° grating with this speed would travel 0.4°, or 0.1 times the radius of the stimulus, during the presentation of the stimulus. In a 2 c/° grating a particular cycle would travel 0.4 times the radius of the pattern. An example trial is illustrated in Movie 2.

The amplitude of the spatial RF pattern test stimulus was varied on a trial by trial basis to sample 9 points on the psychometric function. The point of subjective equality (perception of a circular spatial RF test pattern) equates the after effect due to the adapting motion RF pattern with the amplitude of the spatial RF pattern test stimulus. Results are presented in Figure 3.

Observers have a tendency to see a circle as an RF3 pattern resting on a side but for the 2 c/° adaptor all observers displayed a consistent opposite phase after effect in excess of this bias. However, the 8 c/° adaptor has a weak influence under these conditions. The 8 c/°

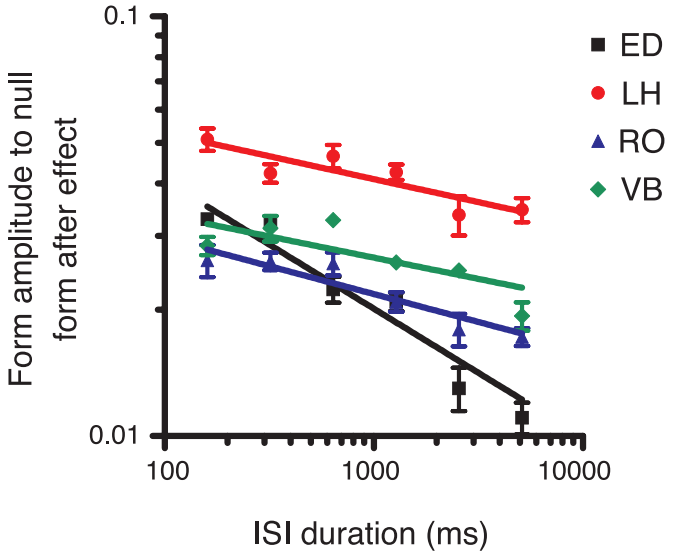

Figure 2. Rate of decay of the spatial form adaptation effect. The graph shows the amplitude of the spatial RF pattern test stimulus required to null the after effect induced by adaptation to a spatial RF pattern of the same phase as a function of the duration of the inter-stimulus interval. The adaptation effect shows a slow decay conforming to a power function.

Movie 2. An example trial from Experiment 2. After adapting to a motion RF pattern a subsequently displayed circle of Gabor patches appears deformed into a spatial RF pattern with the opposite phase of modulation to the motion RF pattern.

patterns might be expected to show a smaller effect than the 2 c/° patterns for a number of reasons: The extrapolated distance traveled by a cycle of modulation during the presentation of the adaptor is smaller by a factor of 4; the size of each Gabor patch is small in comparison with the radius of the stimulus, constraining the possible magnitude of the motion position illusion as a ratio of the pattern radius; the preferred spatial frequency of the motion system is lower for higher eccentricities. For these reasons 2 c/° gratings were used for the following experiments, except for Experiment 5 where a direct comparison is made with Rainville and Wilson (2004) and a smaller pattern radius of 2° and 8 c/° gratings were used. The smaller pattern radius used in Experiment 5 results in local positional displacements representing a larger proportion of the radius.

Perceived positional shifts after adaption to motion have also been attributed to the motion after effect (MAE) (Nishida & Johnston, 1999; Snowden, 1998). Such shifts would produce an anti-phase after effect in a circular pattern after adaptation to a motion RF pattern. The cited studies, however, used much longer adaptation times and larger adapting velocities, and also report that the MAE was experienced. The observers in this study did not report perceiving the MAE and although studies have shown that perceived positional displacement can be observed in the absence of the experience of the MAE (McGraw, Whitaker, Skillen, & Chung, 2002) perception of the MAE would be expected for the tangential arrangement of the gratings of the patches in the test patterns of this study. In Experiment 3 the roles of the motion RF pattern and spatial RF pattern as adaptor and test stimuli are reversed eliminating the possibility of any influence of the MAE.

Experiment 3: Brief exposure to a spatial RF pattern results in an after effect with the capacity to null the apparent deformation of a motion RF pattern of the same phase of modulation

The third experiment was essentially the reciprocal of the second. A spatial RF adapting stimulus was shown prior to a motion RF pattern test stimulus. However, because the form RF after effect has been shown to emerge rapidly the amplitude of the adapting spatial RF pattern was varied on a trial by trial basis. A range of speed conditions for the motion RF patterns were tested for two adaptor durations. Rainville and Wilson (2004, 2005) did not systematically examine the effect of duration of the motion RF pattern on perception of the stimulus. Their thresholds for detection are expressed as the amplitude of the sinusoidal speed modulation, yet the subjective experience of a motion RF pattern is of a form deformation that grows in magnitude with duration of the stimulus. This is

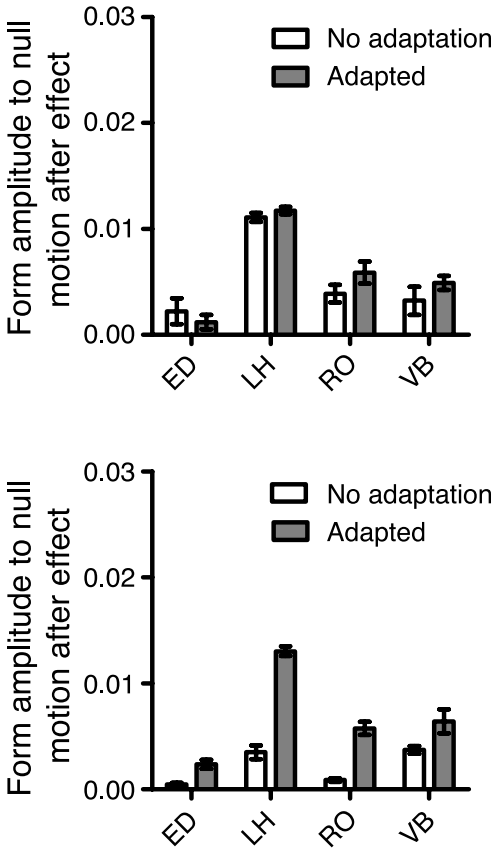

Figure 3. Amplitude of a spatial RF pattern required to null the after effect induced by adaptation to a motion RF pattern of the same phase. The results of the un-adapted conditions demonstrate a tendency of all observers to see a circular stimulus as slightly distorted towards a triangle resting on its base. The after effect induced by the 2 c/° adaptor is larger than for the 8 c/° adaptor. Reported errors are 95% confidence intervals.

Movie 3. An example trial from Experiment 3. An adapting spatial RF pattern is presented for 160 ms. A subsequently presented motion RF pattern has the capacity to null the after effect due to a spatial RF pattern of the same phase of modulation. The judgment of phase is made at the end of the motion RF pattern presentation.

exactly the percept that would be expected if the perceived motion RF pattern deformation were due to the motion position illusion. Up to a limit which is defined by the properties of the stimulus the magnitude of the perceived displacement has been shown to increase linearly with stimulus duration (Arnold, Thompson, & Johnston, 2007).

For the conditions of this experiment a spatial RF pattern was presented as an adaptor. Initially the test pattern, a motion RF pattern, appears deformed in opposite phase to the adaptor. During the presentation of the test pattern the perceived deformation amplitude decreases to zero and can increase again in the same phase as the adaptor. No perceptual discontinuity is evident as the pattern passes through zero amplitude, as might be expected if the deformation in the opposite phase to the adaptor was due to the form system and deformation in the same phase due to the motion system. This observation suggests that a single global mechanism is at work integrating the perceived local positions of the patches and that these local perceived positions are displaced from their veridical position by the influence of the adaptor and the motion position illusion independently. This experiment was designed to allow the magnitudes of the spatial RF after effect and the motion RF pattern test stimulus to be equated over a range of spatial RF pattern adaptor deformation amplitudes and motion RF pattern speed modulation amplitudes, for two different durations of motion RF pattern test stimuli. For each condition the method of constant stimuli was applied using nine adaptor spatial RF pattern amplitudes. The point of subjective equality, arrived at by fitting a cumulative normal distribution to the psychometric data, represented the spatial RF pattern amplitude required to produce a spatial after effect that nulls the perceived distortion due to the speed modulation of the motion RF pattern at the end of the motion RF stimulus presentation. An example trial is illustrated in Movie 3.

Results are presented in Figure 4. For this experiment the 2 c/° stimulus was used which allowed a greater range of speeds than the 8 c/° stimulus. The maximum speed for the gratings of the Gabor patches in the condition where the speed multiplier was 1 was again 2.288 cycles per second, corresponding to 1.144°/s. The amplitude of the speed modulation increases linearly on the x axis of Figure 4.

For observers ED and LH a point of subjective equality was found for a wide range of velocities equating the after

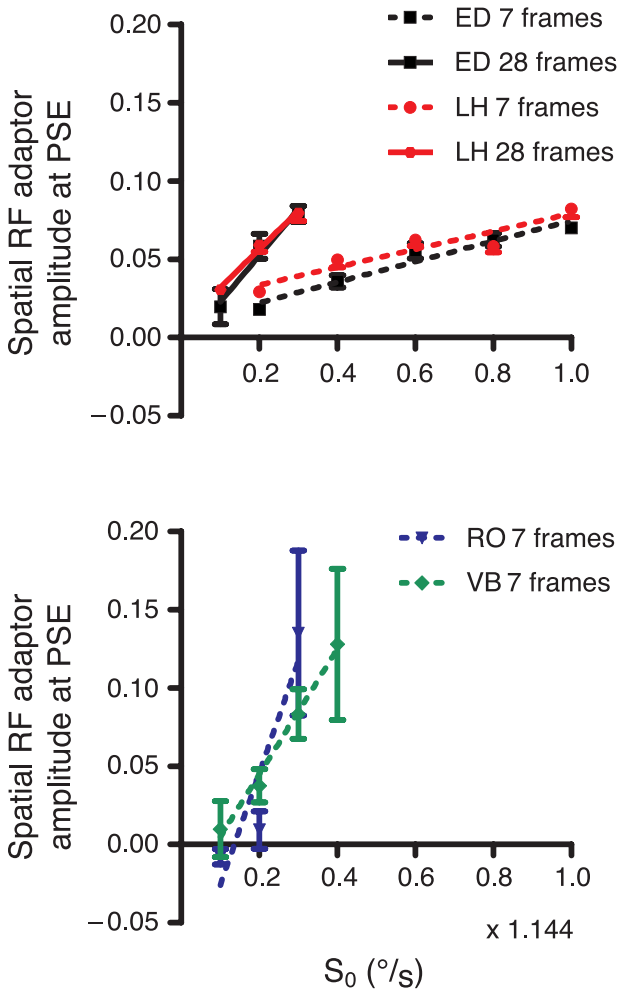

Figure 4. Spatial RF pattern adaptor amplitudes required to produce after effects which equate to (null) specific motion RF pattern amplitudes. As the maximum speed within the motion RF test stimulus increases the adaptor amplitude required to produce a nulling form after effect increases proportionally. The nulling adaptor amplitude also increases in proportion to the duration of the motion stimulus. Error bars represent 95% confidence intervals.

effect due to adaptation to spatial RF patterns and the perceived distortion of motion RF patterns. As the speed modulation amplitude of the motion RF patterns increased, the amplitude of the spatial RF pattern required to produce a motion after effect equal in magnitude to the distortion due to the speed modulation increased proportionally. For these two observers two types of motion stimuli were used. One had 28 frames giving a stimulus duration of 1.4 seconds while the other only had 7 frames resulting in a stimulus duration of 0.35 seconds. The graph shows that the longer motion stimulus had a proportionally larger effect. It is clear then that stimulus duration could be traded for speed. A stimulus with a duration of 7 frames but with four times the amplitude of speed modulation as a 28 frame stimulus would have approximately the same capacity to null the after effect of adaptation to a spatial RF pattern. The magnitude of the perceptual displacement is a linear function of both speed and stimulus duration. The magnitude of the motion position illusion has also been shown to increase with speed and stimulus duration (Arnold et al., 2007; Chung, Patel, Bedell, & Yilmaz, 2007). For two of the observers, RO and VB, the motion stimulus had a much larger effect and it was not possible to arrive at a point of subjective equality between the form induced after effect and the longer duration motion stimulus. Results for these two observers are reported for lower speed conditions of the 7 frame motion stimulus. Experiments 2 and 3, then, demonstrate phase specific after effects of adaptation to motion RF pattern stimuli in spatial RF patterns and vice versa. Experiment 4 tests whether the function describing the perceived positional displacement of a patch with speed of the grating differs across conditions where the test patch is solitary or is incorporated into a motion RF pattern.

Experiment 4: The rate of change of perceived displacement of a Gabor patch with speed of the moving grating is independent of whether the patch is or is not incorporated into a motion RF pattern

De Valois and De Valois (1991) showed that a discrete Gabor patch is perceived as displaced in the direction of motion of its windowed grating and Hayes (2000) showed that the apparent rather than the veridical position predicts the binding of a patch into a path. The motion RF pattern is by definition a path and so the form manifest in the pattern should be reflected in the perceived position of each patch. The results of Experiment 3 imply that the amplitude of the perceived form modulation of a motion RF pattern of a specific duration is a linear function of the amplitude of the speed modulation. This experiment examined the relationship between perceived displacement of a Gabor patch and the speed of its grating, in the conditions where the patch was solitary and where it was incorporated into a motion RF pattern.

This experiment directly measured the magnitude of the displacement of the perceived position of a Gabor patch from its actual position induced by motion of its grating. Measurements were made on a solitary test patch and also on a test patch incorporated into a motion RF pattern. The perceived position of the test patch was measured relative to two vertically arranged external markers 5° above and below the horizontal diameter of the test patch. A fixation point was introduced at the center of the screen such that the test patch was always at an eccentricity of 4° of visual angle and to the right of the fixation point. The stimulus incorporating the 2 c/° patches was used for this experiment and the phase of the motion RF pattern was $\pi/2$ radians, causing the test patch to have the maximum speed in the motion RF pattern. Movie 4 is an example trial of the solitary patch condition. In Movie 5 the same test patch is incorporated into a circular path of Gabor patches.

The maximum speed amplitude (S_0) tested (a value of 1 on the x axis) was 2.288 wavelengths per second, which corresponds to 1.144°/s. The motion stimulus comprised seven 50 ms frames, so the extrapolated distance traveled by a single cycle of a grating with this speed was 0.1 times the radius of the pattern. The observer was required to report whether, at the end of the motion sequence, the test patch appeared to be to the right or left of an imaginary line joining the two reference patches. The reference patches were displaced horizontally on a trial by trial basis and seven points sampled on the psychometric function. A point of subjective alignment was found over a range of speed amplitudes for the two types of pattern. The results are displayed in Figure 5.

The gradients of the lines describing the apparent positions of the patches when they are and are not incorporated into an RF path are not significantly different

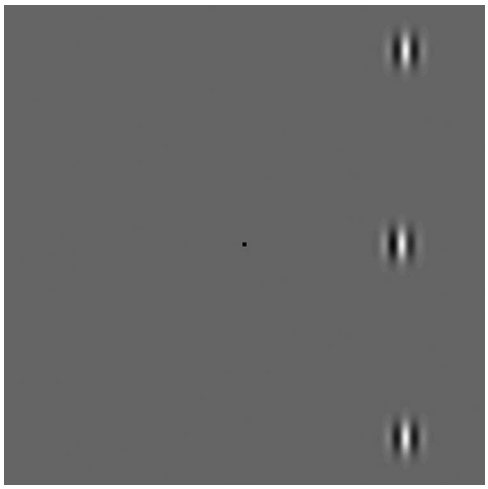

Movie 4. An example of a trial from the solitary patch conditions of Experiment 4. The task of the observer was to report whether the center of the test patch appeared to be to the left or right of an imaginary line joining the centers of the two reference patches, while fixating the dark dot at the center of the screen.

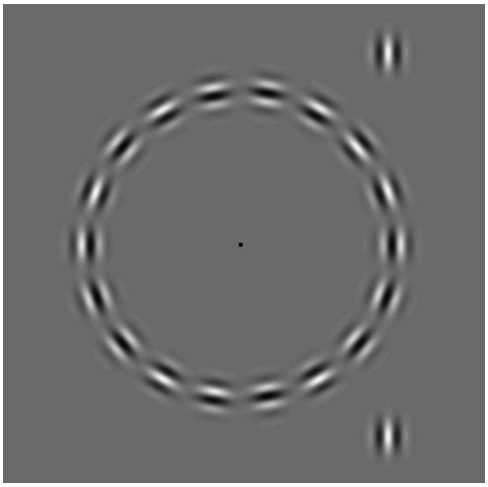

Movie 5. An example trial from the condition of Experiment 4 where the test patch (at θ = 0°) is incorporated into a motion RF pattern. The task of the observer was again to report whether the center of the test patch was to the left or right of an imaginary line joining the centers of the two reference patches.

(ED: $F(1,7) = 1.599$, $p = 0.2466$, VB: $F(1,7) = 0.59$, $p = 0.4675$). The parameter on the y-axis of Figure 5 is the ratio between the perceived displacement of the test patch and the radius of the RF pattern. It represents the apparent spatial modulation of the motion RF pattern as the dimensionless Weber fraction conventionally used to express the deformation of a spatial RF pattern. The gradient of the fitted linear function therefore allows the prediction of the perceived spatial modulation amplitude given the speed modulation amplitude of the motion RF pattern. The pooled gradient of the fitted straight line function is 0.079 per °/s for ED and 0.047 for VB (the Weber fraction is dimensionless and the units of speed modulation are °/s) or 90% and 54% of the extrapolated displacement of a cycle of the grating over the duration of the stimulus respectively. The displacement is a linear function of speed and so a sinusoidal modulation of speed would result in a sinusoidal modulation of apparent position. Spatial RF pattern discrimination threshold for subject SR, reported in Figure 2 of Rainville and Wilson (2004), is approximately 0.005 (random phase). Motion RF pattern threshold for a complete pattern is reported as approximately 0.06°/s (Figure 4: Motion Amplitude Threshold multiplied by 1.92°/s). The ratio between these numbers is 0.083 which is within a factor of 2 of the gradients reported for both ED and VB above, even before correcting for differences in durations between the two stimuli. This result shows that the motion position illusion can account for a large proportion of the perceived deformation of motion RF patterns. This result does not account for the steep slope found by Rainville and Wilson describing integration of coherent motion information around a progressively larger proportion of the path of Gabor patches. However, the reference pattern used by Rainville and Wilson is a version of the test pattern with the speeds of the patches permuted. Panels D, E and F for Figure 3 of Rainville and Wilson (2005) show that when the observer is given prior knowledge of where the coherent sector of motion will appear in a motion RF pattern, thresholds do not increase as the length of the incoherent sector increases. This is indicative of discrimination of coherence in motion direction from incoherent motion over a small sector of the pattern, a local solution. When the observer has no prior knowledge of the position of the coherent sector of motion the threshold increases rapidly towards a condition where the task is not possible. This appears to be the condition at which half of the path has incoherent motion. If the task were being performed locally then

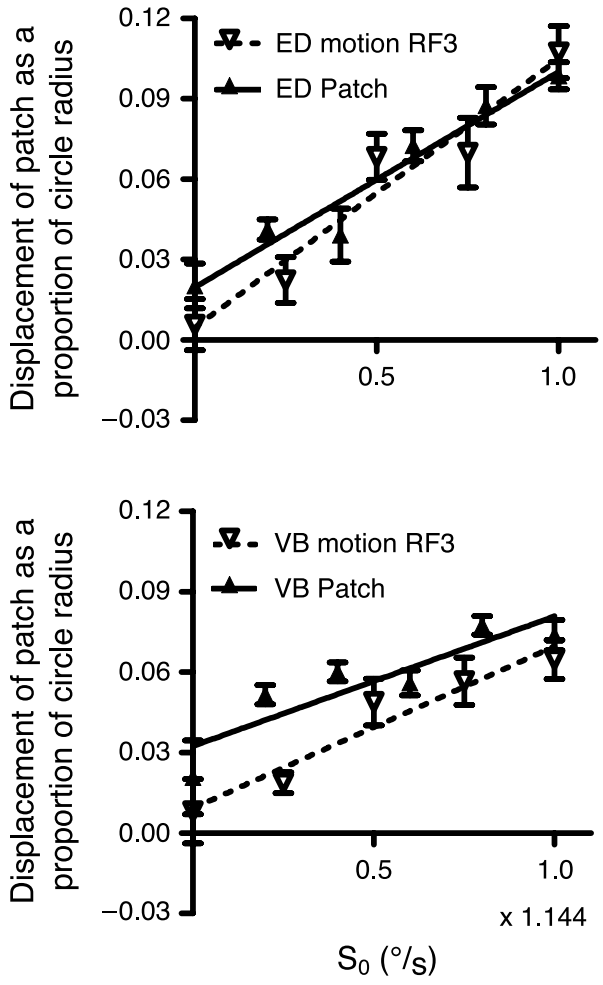

Figure 5. Perceived lateral displacement of a Gabor patch from veridical over a range of grating speeds. Results are presented for conditions where the patch was solitary or was incorporated into a motion RF pattern. Error bars represent 95% confidence intervals. The perceived displacement of a Gabor patch from veridical, expressed as a proportion of its eccentricity (the radius of the motion RF pattern) is plotted against the speed of the grating within the patch. The fitted functions are linear, consistent with the results of Experiment 3, and the rate of change of the perceived displacement with speed is the same for each condition.

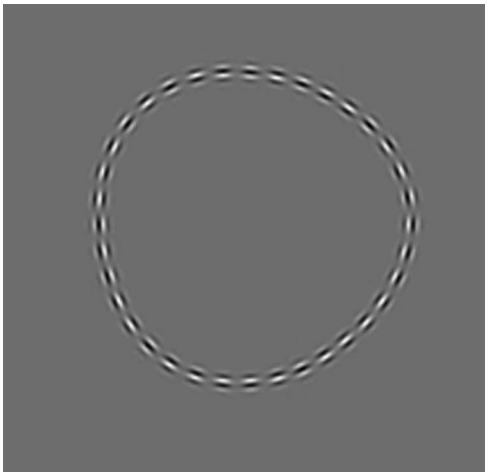

Movie 6. An example trial from Experiment 5 examining sensitivity to spatial RF patterns. The observer was required to report the interval which contained the modulated pattern, a two interval forced choice (2IFC) task.

when half of the path contained incoherent motion the observers would perform at chance for trials where they made their judgment using a sector of the path where both the test and reference stimuli were incoherent. If they performed perfectly when using a sector of the path where the test was coherent then overall they would have a 75% discrimination success rate, the threshold criterion. The condition where half of the path was coherent therefore represents a limit to performance of the task.

Experiment 5 was performed to compare motion RF pattern and spatial RF pattern discrimination thresholds in patterns where local coherence of motion direction could not be used as a cue to discriminate the test and reference stimuli. A d.c. component of centrifugal speed was added to all the elements of the RF patterns allowing cycles of speed modulation to be added one at a time without introducing static or incoherent segments of motion to the test or reference stimuli.

Experiment 5: In the absence of local motion direction cues the summation index across multiple lobes of RF patterns is the same for motion and spatial RF patterns

Experiment 5 is a replication of the summation experiments performed by Rainville and Wilson (2004) but with d.c. component of speed ($S_{d.c.}$) added to all stimuli. A d.c. speed component of 0.5°/s was chosen so that all of the gratings moved centrifugally, precluding the use of a local motion direction discontinuity cue to subvert the task for the motion RF pattern stimuli. The stimuli comprised 12 frames of 40 ms duration each. The spatial frequency of the gratings of the Gabor patches was 8 c/° and each RF path was composed of 36 patches. In the spatial RF patterns the gratings of all patches had a speed of 0.5°/s radially outward and the radius of the pattern was modulated. For the motion RF patterns the patches were arranged on a circle and the speed of the gratings within the patches was modulated above and below the d.c. speed component. In the reference stimuli the radii and speeds were un-modulated. The phases of the RF patterns were randomized. In all conditions the observer was presented with the test and reference stimuli sequentially, in randomized order, and was required to report which of the two stimuli appeared deformed from circular. Conditions using 1, 2 and 3 cycles of modulation of motion and spatial RF3 patterns were examined. Movies 6 and 7 show example trials of a spatial RF pattern and motion RF pattern sensitivity measurements of Experiment 5.

The method of constant stimuli was applied to the two interval forced choice task sampling 7 points on the psychometric function. Quick functions (Quick, 1974) were fitted to the data and the 75% correct performance level adopted as the threshold for discrimination. In order to be able to make a meaningful comparison of the sensitivities to the spatial and motion RF patterns the sensitivities to the motion RF patterns were converted into spatial amplitudes (as a ratio of the radius of the pattern) using the results of an experiment similar to the single patch condition of Experiment 4, but using dimensions pertinent to the stimuli of Experiment 5. The reference patches were 2.5° above and below the test patch which was at an eccentricity of 2° to the right of the fixation point. The spatial frequency of the patches was 8 c/° and the stimulus comprised twelve 40 ms frames. An example stimulus is presented in Movie 8. Movie 9 is an example stimulus within which the patches defining the stimulus

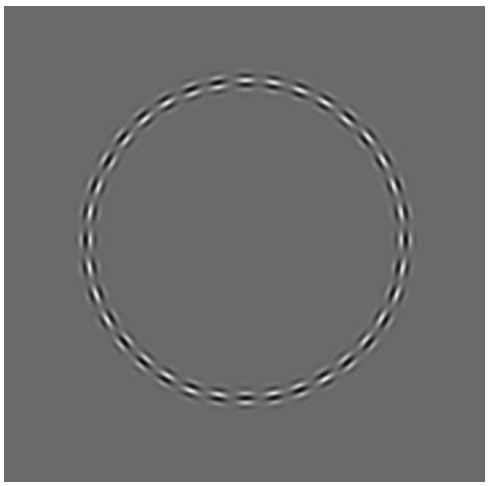

Movie 7. An example trial from the task examining sensitivity to motion RF patterns in Experiment 5. The observer was required to report the interval which contained the modulated pattern. It is evident in the movie that the perceived amplitude of form modulation increases during presentation of the speed modulated stimulus. The perceived size of both stimuli increases.

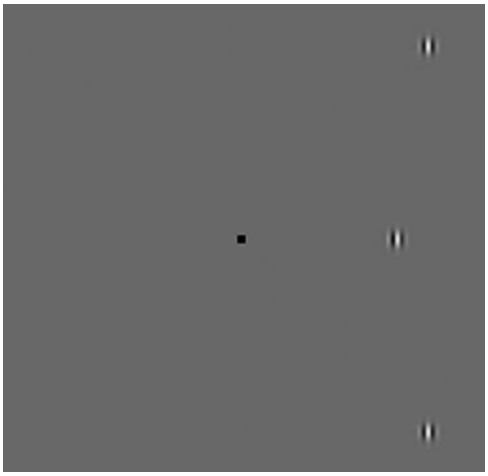

Movie 8. An example trial from an alignment task of Experiment 5 used to derive the transfer function relating grating speed and perceived patch displacement. The task of the observer was to report whether the central target patch was to the left or right of an imaginary line between the two reference patches. Measurements of the magnitude of the motion position illusion versus grating speed provided the transfer function relating the perceived spatial modulation of motion RF patterns due to the modulation of speed around the path. In this example the background had a luminance of 45 cd/m^2. Maximum Michelson contrast of the test patch was 1 and the test patch had a Gaussian luminance profile. A substantial displacement in perceived position develops during the stimulus presentation.

have hard edges and the background has a luminance of <0.5 cd/m^2. The functions describing the perceived displacement versus speed were mapped for both types of stimuli. The results are displayed in Figure 6.

The results displayed in Figure 6 are very different for the two types of stimuli in the alignment tasks. For the stimuli composed of Gaussian windowed gratings the perceived displacement of the patch increased with speed of the grating. Linear functions were fitted to the data of the three observers (solid fitted function lines in Figure 6). The motion position illusion is characterized by the gradient of the line. The non-zero intercepts cannot be related to motion as speed is zero at the intercept. They indicate a perceived distortion of lines in the visual field that do not pass through the fovea and are probably related to the Helmholtz checkerboard illusion (Oomes, Koenderink, van Doorn, & de Ridder, 2009). The gradients of the functions (ED: 13.02′ per °/s, VB: 5.97′ per °/s and JB: 10.15′ per °/s) were used to predict the amplitude of perceived spatial modulation due to the motion position illusion present in the motion RF patterns at their discrimination thresholds. For the stimuli composed of patches with hard edges on a background of near-zero luminance (see Movie 9) the motion position illusion is suppressed (dashed lines in Figure 6). This difference has previously been shown to be true of regions of dots moving coherently within a window cut out of a stationary random dot pattern (Ramachandran & Anstis, 1990). Edges of the window which were defined solely by the contrast in speed of the moving and stationary dots were perceived as displaced in the direction of motion of the dots, while edges which also contained an introduced average luminance difference cue did not. The luminance cue at the hard edge of the Gabor patch suppresses its illusory displacement. This result allowed a direct test of the hypothesis that the form evident in motion RF patterns is due to the motion position illusion. An attempt was made to determine the threshold for discrimination of motion RF patterns from circular patterns in stimuli composed of hard edged patches on a background of near-zero luminance, using the same procedure as for the stimuli composed of Gabor patches. An example stimulus is presented in Movie 10.

No form is evident in the test motion RF pattern displayed as Movie 10. The results of all of the sensitivity experiment are presented together in Figure 7.

Thresholds were determined for 1, 2 and 3 cycles of modulation of spatial and motion RF patterns. Power functions were fitted to these data. The indices describing the power functions are all slightly greater than −1 (Spatial modulation; ED = −0.74, VB = −0.68, JB = −0.74: Speed Modulation; ED = −0.96, VB = −0.68, JB = −0.74). The thresholds predicted due to probability summation across independent local detectors are plotted as dashed lines for comparison. The magnitudes of the slopes of these lines were derived by taking the reciprocal of the average slope of Quick functions fitted to the psychometric data for each of the conditions (Quick, 1974; Wilson, 1980). The fitted functions are steeper than the probability summation threshold prediction lines in all of the 6 cases, suggesting an additive integration of the effect of increasing cycles

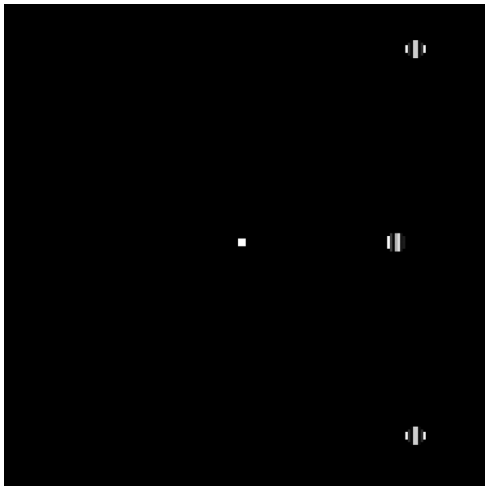

Movie 9. An example trial from an alignment task of Experiment 5 within which the motion position illusion is suppressed. In this stimulus the patches have hard edges and the background luminance is <0.5 cd/m^2. No motion position illusion develops during the presentation of this stimulus.

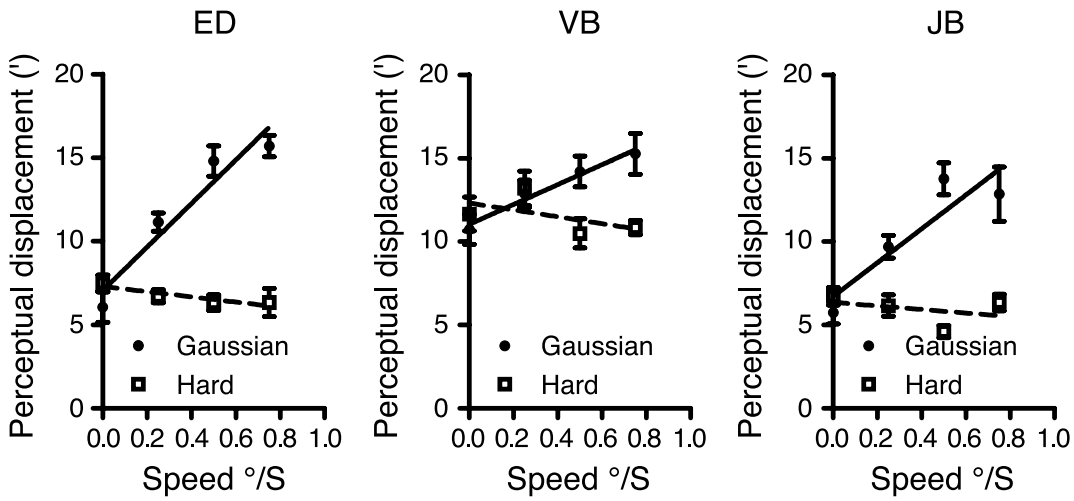

Figure 6. Results of the alignment task relating the magnitude of the motion position illusion in a single patch and speed of the grating. The functions described by the solid and dashed lines relate the perceived displacement of the test patch laterally from veridical as a function of the speed of the gratings in the conventional Gaussian windowed stimuli (see Movie 8) and the hard edged stimuli on a dark background (see Movie 9) respectively.

of modulation (Loffler et al., 2003). The indices of the power functions for the spatial and motion RF patterns are comparable. For two of the three observers the sensitivity to motion RF patterns can be accounted for wholly by the predicted spatial modulation due to the motion position illusion. For observer VB the predicted spatial modulation of the patterns due to the motion position illusion is inadequate to account for the perceived thresholds. The transfer function relating perceived displacement of the patch and speed was shallower for observer VB than for observers ED and JB (see Figure 6) suggesting that the motion position illusion for this observer might have been compromised by a tendency to fixate nearer to the test patch than the other observers, reducing the magnitude of the illusion. It is clear, however, that the motion position illusion has the potential to account for a large proportion of the sensitivity to motion RF patterns. The lack of any perceived deformation in motion RF patterns composed of hard edged patches on a dark background, at amplitudes approaching an order of magnitude higher than thresholds for the patterns composed of Gabor patches, confirms that in the absence of the motion position illusion deformation is not perceived.

Discussion

The stimulus devised by Rainville and Wilson (2004, 2005) is a path of Gabor patches. In the null stimulus the centers of the Gaussian windows of the Gabor patches lie on a circular path and their gratings are stationary and tangential to the path. This null stimulus can be manipulated in two ways. In the spatial manipulation of the stimulus the positions of the Gabor patches are modulated sinusoidally from the circular path with the gratings remaining tangential to the path. Earlier experiments have shown observers to be extremely sensitive to such spatial RF deformations in continuous contours (Bell et al., 2007; Loffler et al., 2003; Wilkinson et al., 1998). The motion manipulation of the stimulus involves introducing a sinusoidal radial speed distribution to the gratings of the

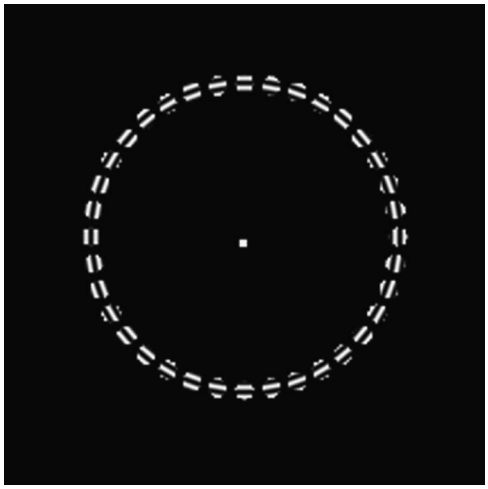

Movie 10. An example trial used in a sensitivity experiment of Experiment 5 performed to measure the perceived deformation of motion RF patterns that exhibit no motion position illusion. The speed modulation amplitude of the test pattern of the pair of stimuli is 0.2°/s, which is substantially larger than the threshold for discrimination of test from reference motion RF patterns composed of Gabor patches on a background of 45 cd/m^2. No form deformation is present in the test stimulus and neither the test nor reference stimuli appear to grow in radius.

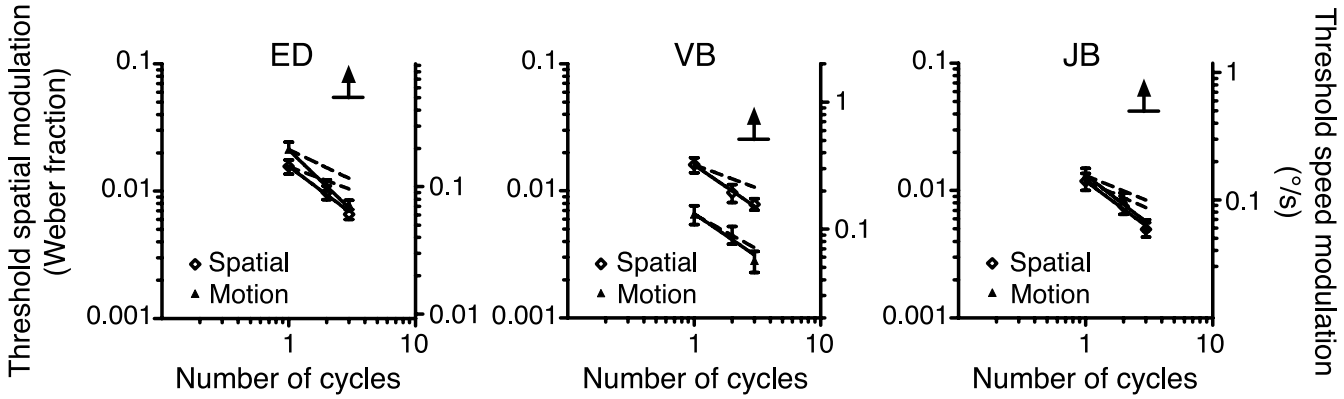

Figure 7. Comparison of threshold amplitudes for discrimination of spatial and motion RF patterns from circular reference stimuli. Discrimination thresholds for spatial RF patterns with 1, 2 and 3 cycles of modulation are plotted with reference to the left y axis and thresholds for motion RF patterns to the right y axis. The left and right y axes have been aligned using the motion position illusion transfer function for each observer. Solid lines are fitted power functions and the dashed lines thresholds predicted by probability summation. The bar with the upward pointing arrow represents the lower limit for the un-measurable threshold for discrimination of a motion RF pattern from a reference for the condition with the hard edged patches and dark background.

Gabor patches. Sensitivity to this manipulation implies either that the visual system is sensitive to a sinusoidal modulation of radial speed in the absence of a spatial deformation cue, or that local motion introduces an apparent displacement to each of the Gabor patches in the direction of the motion, which is interpreted by the form system as a distortion of the path. Rainville and Wilson (2004, 2005) favored the first of these interpretations citing evidence that motion RF modulation pedestals had a detrimental effect on discrimination thresholds for spatial RF deformation both in phase and out of phase with the test pattern modulation. However, the perceived form of a motion RF pattern has amplitude maxima at the points where the motion is maximally centrifugal and spatial RF patterns have been shown to elicit spatial RF after effects of opposite phase (Anderson et al., 2007) which raises the question of whether motion RF patterns exhibit spatial RF after effects of opposite phase. The spatial RF after effect is independent of the contrast of the adapting stimulus (Anderson et al., 2007) suggesting the neural mechanisms responsible for encoding the shape are downstream of those effecting contrast gain control. Experiment 1 of this study demonstrates that the after effect develops over a very short adaptation period (40 ms) and in the absence of an intervening stimulus the adaptation is persistent in comparison to the rise time. Experiment 2 shows that a spatial RF pattern of the same phase as an adapting motion RF pattern nulls the after effect. Experiment 3 confirms the reciprocal effect, that a motion RF pattern of the same phase as an adapting spatial RF pattern nulls the after effect. The phase specificity and linear relationship between the after effect of adaptation to spatial RF patterns and the percept of the form of the motion RF patterns suggests that the reconciliation of the spatial and motion RF information might occur earlier in the visual system than proposed by Rainville and Wilson. Experiment 4 shows that the perceived displacement of a Gabor patch due to the motion position illusion is related linearly to the speed of the grating in the patch, and is a large proportion of the extrapolated displacement of a single cycle of the grating over the course of the stimulus presentation. This is true for an isolated patch and also for a patch incorporated into a closed path. If the form processing stream of the visual system were to use the perceived positions rather than the actual positions in the analysis of form then the motion in the motion RF patterns would result in the encoding of this deformation in the form system. Experiment 5 tests whether this deformation would be sufficient to account for sensitivity to motion RF patterns. The parameters of the motion RF pattern stimuli used in Experiment 5 approximated those used by Rainville and Wilson but with an additional d.c. component of centrifugal motion to ensure that in all conditions the motion of all patches was in the same direction (centrifugal) to preclude the use of local speed discontinuities to perform the task. Sensitivities to 1, 2 and 3 cycles of deformation of motion RF patterns and spatial RF patterns were compared through the application of a transfer function relating the size of the motion position illusion to grating speed in a patch. The spatial deformation of motion RF patterns at their detection threshold that can be attributed to the motion position illusion is comparable to the thresholds for detection of spatial RF patterns. Moreover, the indices of the power functions describing the decrease in threshold with increasing numbers of cycles of deformation were comparable across motion and form conditions and were indicative of summation of signal across cycles. Also, we showed that no deformation could be perceived in a motion RF stimulus composed of hard edged patches on a dark background, a stimulus which does not support the motion position illusion. The motion position illusion is

therefore necessary for the perception of deformation in motion RF patterns. We conclude that the most parsimonious explanation for the perceived deformation of motion RF patterns is the integration of perceived positions of independent patches displaced in the direction of motion of the gratings within them by an amount proportional to the speed of the gratings. Rainville and Wilson (2004, 2005) rejected this conclusion primarily on the basis that; a) integration over progressively larger numbers of Gabor patches and hence cycles of speed modulation improves sensitivity (the reciprocal of threshold) at a rate which is steeper than linear and b) their measures of the displacement of the perceived positions of Gabor patches with gratings moving at speeds corresponding to the maxima of speed modulation in motion RF patterns at detection threshold was inadequate to produce a spatial RF of detectable amplitude. However data from panels D, E and F of Figure 3 of Rainville and Wilson (2005) suggest that detection of the motion RF patterns in their task (discriminating a pattern with a sector of coherent speeds from a pattern where the speeds have been permuted across patches) is local. The data points represented by unfilled symbols, which represent thresholds for patterns where the position of the coherent sector was known to the observers, show constant rather than reducing thresholds with increasing numbers of coherently moving patches. This suggests that the improvement reported by Rainville & Wilson may have been a consequence of reducing spatial uncertainty when larger sectors of coherently moving patches were presented, rather than global spatial summation. This might also explain the fact that Rainville and Wilson (2004) saw no systematic change in threshold for detection of motion RF patterns across radial frequency (Figure 3 of their paper). Rainville and Wilson (2005) show that motion RF2s can be discriminated from RF3s, and RF3s from RF4s at particular thresholds (panels B and C of Figure 3) when modulation occupies the complete stimulus (threshold increasing sharply when it is not complete). However, as it appears that these data have been normalized within the data set (thresholds for discriminating between the wholly coherent patterns = 1), we cannot compare the thresholds for discrimination between RF patterns with differing frequencies with those for discriminating motion RF patterns from patterns with speeds permuted across patches. It seems possible that in the studies undertaken by Rainville and Wilson observers were most sensitive to local coherence in speed rather than the global speed modulation. This argument does not explain the small displacements in perceived position for control stimuli illustrated in Figure 5 of Rainville and Wilson (2005) at motion RF threshold velocities. However, in the alignment task used to derive their transfer function the target patch and reference patches were part of the same path defined by the Gaussian contrast envelopes of the patches. The gratings of the target and reference patches were in relative motion but the path could be considered to be a kinetic edge (Ramachandran & Anstis, 1990; Ramachandran & Inada, 1985) as average luminance contrast to background is close to zero. Under such circumstances the gratings might be treated as texture and perceived as moving in synchrony. However, perhaps the most compelling evidence that distortion of motion RF patterns is simply the result of a systematic change in the motion position illusion around the pattern is the fact that motion RF patterns composed of patches which do not support the motion position illusion do not appear distorted. Even for speed modulation amplitudes an order of magnitude larger than the threshold for detection of deformation in the typical motion RF patterns the patterns with a dark background and hard edged patches did not show any deformation.

Overall the results of this series of experiments shows that while sinusoidal modulation of speeds can produce a compelling radial frequency contour; the processing of that contour is consistent with local motion position illusions inducing the spatial modulation which is then processed by the same system as spatial RF patterns. At this point there is no need to propose motion equivalents of the global form processes which detect radial frequency contours.

Acknowledgments

This research was supported by Australian Research Council Grant DP0666206 to D.R.B.

Commercial relationships: none.
Corresponding author: James Edwin Dickinson.
Email: edwind@cyllene.uwa.edu.au.
Address: 35 Stirling Highway, Crawley, Perth, WA 6009, Australia.

References

Anderson, N. D., Habak, C., Wilkinson, F., & Wilson, H. R. (2007). Evaluating shape after-effects with radial frequency patterns. *Vision Research, 47,* 298–308. [PubMed]

Arnold, D. H., Thompson, M., & Johnston, A. (2007). Motion and position coding. *Vision Research, 47,* 2403–2410. [PubMed]

Bell, J., & Badcock, D. R. (2009). Narrow-band radial frequency shape channels revealed by sub-threshold summation. *Vision Research, 49,* 843–850. [PubMed]

Bell, J., Badcock, D. R., Wilson, H., & Wilkinson, F. (2007). Detection of shape in radial frequency contours: Independence of local and global form information. *Vision Research, 47,* 1518–1522. [PubMed]

Bell, J., Wilkinson, F., Wilson, H. R., Loffler, G., & Badcock, D. R. (2009). Radial frequency adaptation reveals interacting contour shape channels. *Vision Research, 49,* 2306–2317. [PubMed]

Biederman, I. (1987). Recognition-by-components: A theory of human image understanding. *Psychological Review, 94,* 115–147. [PubMed]

Chung, S. T. L., Patel, S. S., Bedell, H. E., & Yilmaz, O. (2007). Spatial and temporal properties of the illusory motion-induced position shift for drifting stimuli. *Vision Research, 47,* 231–243. [PubMed] [Article]

De Valois, R. L., Cottaris, N. P., Mahon, L. E., Elfar, S. D., & Wilson, J. A. (2000). Spatial and temporal receptive fields of geniculate and cortical cells and directional selectivity. *Vision Research, 40,* 3685–3702.

De Valois, R. L., & De Valois, K. K. (1991). Vernier acuity with stationary moving Gabors. *Vision Research, 31,* 1619–1626. [PubMed]

Field, D. J., Hayes, A., & Hess, R. F. (1993). Contour integration by the human visual system: Evidence for a local "association field". *Vision Research, 33,* 173–193. [PubMed]

Hayes, A. (2000). Apparent position governs contour-element binding by the visual system. *Proceedings of the Royal Society of London B: Biological Sciences, 267,* 1341–1345. [PubMed] [Article]

Hubel, D. H., & Wiesel, T. N. (1968). Receptive fields and functional architecture of monkey striate cortex. *The Journal of Physiology, 195,* 215–243. [PubMed]

Keeble, D. R. T., & Nishida, S. (2001). Micropattern orientation and spatial localization. *Vision Research, 41,* 3719–3733. [PubMed]

Kovacs, I., & Julesz, B. (1993). A closed curve is much more than an incomplete one: Effect of closure in figure-ground segmentation. *Proceedings of the National Academy of Sciences of the United States of America, 90,* 7495–7497. [PubMed] [Article]

Li, W., & Gilbert, C. D. (2002). Global contour saliency and local colinear interactions. *Journal of Neurophysiology, 88,* 2846–2856. [PubMed] [Article]

Loffler, G., Wilson, H. R., & Wilkinson, F. (2003). Local and global contributions to shape discrimination. *Vision Research, 43,* 519–530. [PubMed]

McGraw, P. V., Whitaker, D., Skillen, J., & Chung, S. T. L. (2002). Motion adaptation distorts perceived visual position. *Current Biology, 12,* 2042–2047. [PubMed]

Nachmias, J., & Sansbury, R. V. (1974). Letter: Grating contrast: Discrimination may be better than detection. *Vision Research, 14,* 1039–1042. [PubMed]

Nishida, S. y., & Johnston, A. (1999). Influence of motion signals on the perceived position of spatial pattern. *Nature, 397,* 610–612. [PubMed]

Oomes, A. H. J., Koenderink, J. J., van Doorn, A. J., & de Ridder, H. (2009). What are the uncurved lines in our visual field? A fresh look at Helmholtz's checkerboard. *Perception, 38,* 1284–1294.

Quick, R. F., Jr. (1974). A vector-magnitude model of contrast detection. *Kybernetik, 16,* 65–67. [PubMed]

Rainville, S. J. M., & Wilson, H. R. (2004). The influence of motion-defined form on the perception of spatially-defined form. *Vision Research, 44,* 1065–1077. [PubMed]

Rainville, S. J. M., & Wilson, H. R. (2005). Global shape coding for motion-defined radial-frequency contours. *Vision Research, 45,* 3189–3201. [PubMed]

Ramachandran, V. S., & Anstis, S. M. (1990). Illusory displacement of equiluminous kinetic edges. *Perception, 19,* 611–616. [PubMed]

Ramachandran, V. S., & Inada, V. (1985). Spatial phase and frequency in motion capture of random-dot patterns. *Spatial Vision, 1,* 57–67. [PubMed]

Regan, D., & Hamstra, S. J. (1992). Dissociation of orientation discrimination from form detection for motion-defined bars and luminance-defined bars: Effects of dot lifetime and presentation duration. *Vision Research, 32,* 1655–1666. [PubMed]

Snowden, R. J. (1998). Shifts in perceived position following adaptation to visual motion. *Current Biology, 8,* 1343–1345. [PubMed]

Wilkinson, F., Wilson, H. R., & Habak, C. (1998). Detection and recognition of radial frequency patterns. *Vision Research, 38,* 3555–3568. [PubMed]

Wilson, H. R. (1980). A transducer function for threshold and suprathreshold human vision. *Biological Cybernetics, 38,* 171–178. [PubMed]